The British Journal of Radiology, 85 (2012), 225–230

Appearances of colorectal hepatic metastases at diffusion-weighted MRI compared with histopathology: initial observations

[1]E D SCURR, BSc, MSc, [2]D J COLLINS, BA (Hons), MInstP, [3]L TEMPLE, FRCPath, [4]N KARANJIA, FRCS, [2]M O LEACH, PhD and [1]D-M KOH, FRCR, MRCP

[1]*Department of Radiology, Royal Marsden Hospital, Sutton,* [2]*CR-UK and EPSRC Cancer Imaging Centre, Institute of Cancer Research and Royal Marsden Hospital, Sutton,* [3]*Department of Pathology, Epsom General Hospital, Epsom, and* [4]*Department of Surgery, Royal Surrey County Hospital, Guildford, UK*

Objective: To describe the appearances of colorectal liver metastases on diffusion-weighted MRI (DW-MRI) and to compare these appearances with histopathology.
Methods: 43 patients with colorectal liver metastases were evaluated using breath-hold DW-MRI (*b* values 0, 150 and 500 s mm^{-2}). The $b=500$ s mm^{-2} DW-MRI were reviewed consensually for lesion size and appearance by two readers. 18/43 patients underwent surgery allowing radiological–pathological comparison. Tissue sections were reviewed by a pathologist, who classified metastases histologically as cellular, fibrotic, necrotic or mixed. The frequency of DW-MRI findings and histological features were compared using the χ^2 test.
Results: 84 metastases were found in 43 patients. On $b=500$ s mm^{-2} DW-MRI, metastases showed three high signal intensity patterns: rim (55/84), uniform (23/84) and variegate (6/84). Of the 55 metastases showing rim pattern, 54 were >1 cm in diameter ($p<0.01$, χ^2 test). 25/84 metastases were surgically resected. Of these, 11/22 metastases >1 cm in diameter showed rim pattern and demonstrated central necrosis at histopathology ($p=0.04$, χ^2 test). No definite relationship was found between uniform and variegate patterns with histology.
Conclusion: Rim high signal intensity was the most common appearance of colorectal liver metastases >1 cm diameter on DW-MRI at *b* values of 500 s mm^{-2}, a finding attributable to central necrosis.

Received 25 February 2010
Revised 18 May 2010
Accepted 27 May 2010

DOI: 10.1259/bjr/11597735

The appearances of colorectal liver metastases on contrast-enhanced MRI are well described. Following administration of extracellular gadolinium contrast medium, colorectal liver metastases typically show rim enhancement in the arterial phase, but appear hypointense in the portovenous and interstitial phases of enhancement [1, 2]. Using small iron oxide particles (SPIO), metastases appear hyperintense on T_2* weighted imaging [3, 4]. On mangafodipir trisodium (MnDPDP) [5, 6] or gadoxetic acid (Gd-EOB-DTPA) enhanced imaging [7–9], metastases are hypointense on T_1 weighting in the hepatocellular phase of enhancement.

Diffusion-weighted MRI (DW-MRI) does not require exogenous contrast administration and derives its image contrast from differences in the mobility of water between tissues [10]. In areas where the extracellular space is reduced or the tortuosity of the extracellular space is increased (*e.g.* cellular tumour tissues), the signal intensity on diffusion-weighted images is high, which reflects decreased water diffusivity.

DW-MRI is increasingly applied in the liver for disease detection and characterisation. It has been shown that DW-MRI is more sensitive than T_2 weighted MRI for lesion detection [11, 12]. Furthermore, DW-MRI used on its own or in combination with contrast-enhanced imaging can improve the detection of metastases [13, 14]. Clearly, recognising the range of DW-MRI appearances of colorectal liver metastases would increase the confidence of their diagnosis. DW-MRI may be particularly valuable in patients with renal impairment, in whom there may be reluctance or contraindication to the administration of extracellular gadolinium contrast media.

In our clinical practice, we have observed a range of DW-MRI appearances of colorectal liver metastases, and, although metastases can be detected at *b* values of 150 s mm^{-2}, these demonstrate more characteristic appearances at a higher *b* value of 500 s mm^{-2}. As far as we are aware, the DW-MRI appearances of colorectal liver metastases have not been previously reported in the published literature. Furthermore, the pathological basis for the DW-MRI appearances of colorectal liver metastases has not been clearly established. Radiological–pathological comparisons of colorectal liver metastases can inform our understanding of the histological changes that result in their DW-MRI appearance, and may in future help to identify biologically relevant subgroups for selective treatment. Hence, the aim of this study was to describe the appearances of colorectal liver metastases on DW-MRI and to compare these appearances with histopathology.

Address correspondence to: Dr Dow-Mu Koh, Department of Radiology, Royal Marsden Hospital, Downs Road, Sutton SM2 5PT, UK. E-mail: dowmukoh@icr.ac.uk

Materials and methods

The study was approved by the local research and ethics committee and written informed consent was obtained from all patients prior to enrolment in the study.

Study population

This was a prospective study of 43 patients (26 male and 17 female) with a mean age of 62 years (range 42–78 years). The inclusion criteria were patients with pathologically proven colorectal cancer with radiologically (ultrasound or CT imaging) suspicious or confirmed liver metastases who were referred for MRI to assess surgical resectability of disease (*i.e.* segmental sparing of at least two contiguous Couinard liver segments). The exclusion criteria were: (1) patients with contraindications to MRI and (2) a history of other known primary malignancies.

Of the 43 consecutive patients included in the study, 18 were found to be suitable for surgery and underwent resection following MRI (mean 16.4 days, range 8–32 days), allowing 25 metastases to be directly compared with histopathology. In the remaining 25 patients, 59 metastases were identified. These patients were treated with chemotherapy. Each metastasis showed: (1) at least a 20% increase or decrease in lesion size on follow-up for 6 months while on treatment or (2) increased tracer uptake of 18-fluorodeoxyglucose positron emission tomography prior to treatment, which were taken as evidence of metastatic disease.

Imaging protocol

In patients who underwent liver resection, MRI was performed within 1 week of surgery. In the remaining patients, MRI was performed prior to the start of any treatment. All patients were evaluated on a 1.5 T Philips Intera MR system. Imaging signal-to-noise was maximised by using a four-channel phased-array body coil, centred to the xiphisternum to encompass the whole liver. DW-MRI was performed using breath-hold, single-shot echoplanar imaging with parallel imaging. Axial DW-MRI of the entire liver was performed [repetition time (TR)=1850 ms, echo time (TE)=56–68 ms, 7 mm section thickness, 1 mm gap, matrix=112×256 mm, parallel imaging SENSE factor=2] using three b values (0, 150 and 500 s mm^{-2}) applied in three orthogonal directions of phase, measurement and slice (P, M, S). 12 image sections were acquired in each 20 s breath-hold, and the entire liver was evaluated in typically 2 or 3 breath-holds. For each image section, the trace or index image for the 150 and 500 b value images were generated.

In addition to DW-MRI, unenhanced T_1 weighted (in- and out-of-phase gradient echo technique) and T_2 weighted (turbo spin echo technique with dual echo times of 80 ms and 180 ms) images were also acquired. In line with local imaging practice, T_1 weighted imaging was also performed after MnDPDP contrast administration.

Image interpretation

The b=500 s mm^{-2} trace DW-MRI were reviewed in consensus by two expert readers (both with 5 years' experience of DW-MRI of the liver). Imaging review was performed using a workstation (ViewForum, Philips Medical, Best, the Netherlands). The unenhanced and MnDPDP-enhanced MRIs were available for cross-reference if required. For each metastasis encountered, the following were recorded:

- *Lesion size*. The largest axial diameter of each metastasis was measured using the measurement tool on the workstation and recorded in centimetres.
- *Lesion appearance*. The DW-MRI appearances of colorectal liver metastases were classified on the b= 500 s mm^{-2} images as showing high signal intensity in the periphery of tumours only (*rim* pattern), high signal intensity across the entire lesion (*uniform* pattern) or a variegated high signal intensity appearance (*variegate* pattern) (Figure 1).

Pathological evaluation

Following surgical resection of the liver metastases, the pathological specimens were fixed in formalin. A whole-mount tissue section was obtained through each metastasis at its maximum diameter. When this was not possible (*e.g.* when the metastasis was too large to be accommodated), representative areas were taken from the centre and periphery of each metastasis and mounted onto slides. Histological sections were stained with haematoxylin and eosin and evaluated by an expert histopathologist with more than 10 years' experience. For each metastasis, the dominant histological feature was identified, and metastases were classified as cellular, fibrotic, necrotic or mixed features. A metastasis was classified as cellular if more than two-thirds of the metastasis comprised viable tumour tissue. A metastasis was classified as fibrotic when more than about one-third of the metastasis showed deposition of collagenous fibres or fibroblastic response. A metastasis was classified as necrotic when more than one-third of the lesion showed coagulative or liquefactive necrosis. A metastasis showing mixed features had approximately equal parts of cellular, fibrotic and necrotic features. For metastases classified as fibrotic or necrotic, the location of these changes was recorded as being central or peripheral.

Statistical analysis

Statistical analysis was performed using MedCalc software v.9.5.0 (MedCalc Software, Mariakerke, Belgium). The frequency of the morphological appearance of the metastases (*rim*, *uniform* or *variegate* patterns) on DW-MRI was compared between lesions $\leq$1 cm and $>$1 cm in maximum diameter using the χ^2 test. The frequencies of the DW-MRI appearances of metastases in diameter were also compared with the frequency of the four histological subtypes using the χ^2 test. A $p<0.05$ was taken to be statistically significant.

Results

84 metastases were found in 43 patients. Of these, 25/84 were confirmed by histology following surgery, and the remaining 59/84 were determined to be metastases

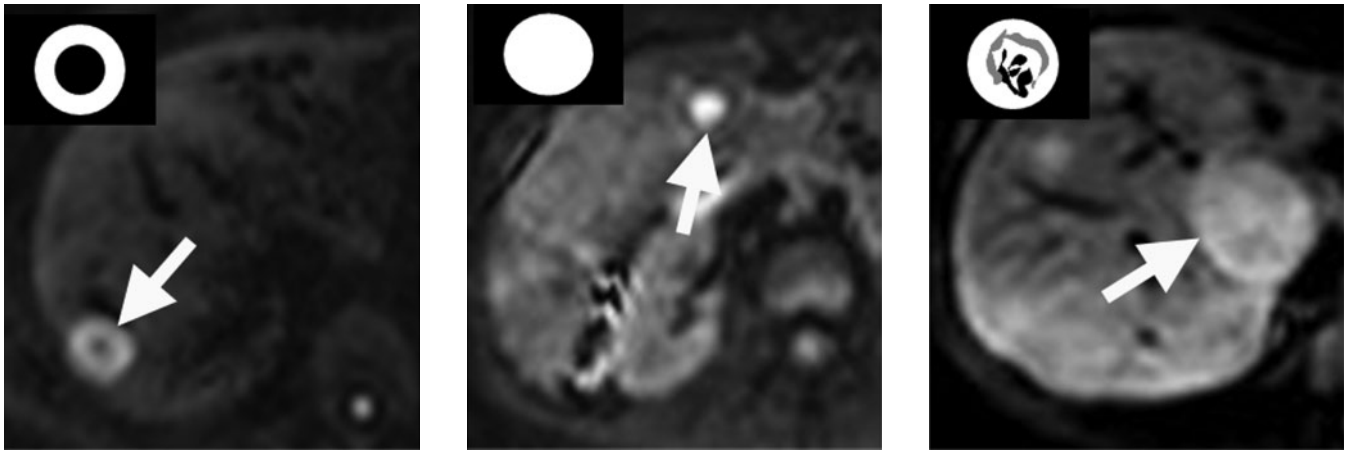

(a) (b) (c)

Figure 1. Diffusion-weighted MRI (DW-MRI) appearances of colorectal liver metastases. DW-MRI (echo time/repetition time=1850/60) acquired at a *b* value of 500 s mm^{-2} (*b*=500) showing the three morphological patterns observed. (a) Rim high signal intensity pattern (arrow) of a metastasis in the right lobe of the liver, characterised by a hyperintense rim but relative hypointense centre. (b) Uniform high signal intensity pattern (arrow) of a metastasis in the right lobe. (c) Variegate high signal intensity pattern (arrow) of a metastasis in the caudate lobe characterised by heterogeneous low and high signal intensity areas within the metastasis.

by follow-up imaging. The mean number of metastases per patient was 1.2 (range 1–6). 15/84 lesions (17.5%) were found in the left lobe of the liver and 69/84 (82.5%) in the right lobe. The mean size of the metastases was 3.1 cm (range 0.5–16.5 cm).

Appearances of colorectal liver metastases on DW-MRI

The morphological appearances of the metastases were as follows: 55/84 (65.5%) exhibited a *rim* appearance, 23/84 (27.4%) of lesions were *uniform* and 6/84 (7.1%) were *variegate*.

The frequencies of the morphological appearances of liver metastases according to whether they were ≤1 cm or >1 cm in maximum diameter are shown in Table 1. 70 metastases measured >1 cm in diameter and 14 were ≤1 cm in diameter. The *rim* pattern was more frequently encountered in metastases >1 cm in diameter ($p<0.01$, χ^2 test). The *uniform* pattern was more frequently encountered in metastases measuring <1 cm in diameter ($p<0.01$, χ^2 test) (Figure 2). Of the 55 metastases that showed a *rim* pattern on DW-MRI, 54 were greater than 1 cm in diameter, whereas 13/23 showing *uniform* appearance were less than 1 cm. The *variegate* pattern was not observed in metastases less than 1 cm in diameter.

Appearances of colorectal liver metastases at histopathology

25 metastases were resected in 18 patients. The mean size of the resected metastases was 2.7 cm (range 0.5–6.0 cm). Of these, 22/25 were >1 cm in diameter and 3/25 were ≤1 cm.

For the 3/25 metastases that were ≤1 cm in diameter, histopathology revealed cellular subtype in 2/25 and necrotic subtype in 1/25. All showed uniform high signal intensity on DW-MRI.

For metastases >1 cm in diameter, the frequencies of the different histological subtypes compared with DW-MRI appearances are summarised in Table 2. The necrotic histological subtype was most frequently encountered (12/22). All necrotic changes were noted to be central rather than peripheral. When compared with the DW-MRI appearances, the necrotic subtype was observed in 11/15 metastases exhibiting the *rim* high signal pattern on DW-MRI ($p=0.04$, χ^2 test) (Figure 3). No significant relationship was found between the *uniform* and *variegate* DW-MRI patterns with the different histopathological subtypes, although 2/4 metastases exhibiting the *uniform* high signal pattern on DW-MRI showed fibrotic appearance at histopathology (Figure 4). In the 4/22 metastases showing fibrotic histology, two showed *uniform* pattern and two showed *rim* pattern. The fibrotic changes were also found towards the centre rather than the periphery of the metastases. There were no mucinous metastases encountered in the surgical cases.

Discussion

Accurate assessment of the presence, location and burden of colorectal liver metastases on a lesion-by-lesion basis is critical for treatment planning. Imaging detection and characterisation of focal liver lesions in patients with colorectal cancer is currently reliant on the use of contrast medium. In this regard, dynamic

Table 1. Frequency of the rim, uniform and variegate high signal intensity patterns of colorectal liver metastases observed on DW-MRI metastases according to lesion size ≤1 cm or >1 cm

DW-MRI appearance at *b*=500 s mm^{-2}	Size of liver metastases ≤1 cm	>1 cm	Total
Rim	1	54	55
Uniform	13	10	23
Variegate	0	6	6
Total	14	70	84

DW-MRI, diffusion-weighted MRI.

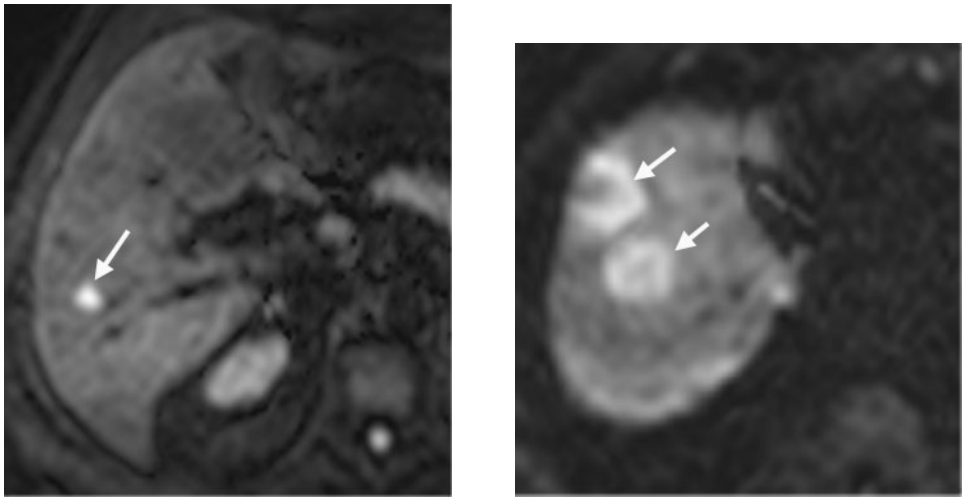

(a) (b)

Figure 2. Diffusion-weighted MRI (DW-MRI) appearances of metastases ≤1 cm and >1 cm in diameter. DW-MRI (echo time/repetition time=1850/60) acquired at a *b* value of 500 s mm^{-2}. (a) Uniform high signal intensity pattern (arrow) was most frequently observed among metastases ≤1 cm in diameter, whereas (b) the rim high signal intensity pattern (arrows) was most frequently seen in metastases >1 cm in diameter.

extracellular gadolinium chelate-enhanced MRI is still the most frequently used, although hepatocyte-selective (*e.g.* gadoxetic acid Gd-EOB-DTPA) and other liver-specific contrast media (*e.g.* superparamagnetic iron oxide, MnDPDP) may be utilised in addition to, or in preference to, extracellular gadolinium chelates depending on local practice and experience.

DW-MRI, which does not require contrast administration, has been shown to aid lesion characterisation in the liver. DW-MRI can help to distinguish solid from cystic lesions, although differentiating between different solid hepatic lesions is challenging based on visual assessment of the high *b* value DW-MRI alone. This is because most solid hepatic lesions, whether benign or malignant, show variable degrees of high signal intensity impeded diffusion on DW-MRI. However, in a study population with a very high pre-test probability of colorectal liver metastases or when liver metastases have already been demonstrated by other imaging techniques (*e.g.* CT or ultrasound), a solid hepatic lesion encountered on DW-MRI could be considered as highly suspicious for metastatic disease. Nevertheless, knowledge of the imaging appearances of colorectal liver metastases on DW-MRI could also add confidence to the recognition and detection of metastatic disease, especially when the administration of contrast material is contraindicated.

Table 2. Frequency of rim, uniform and variegate high signal intensity patterns of colorectal liver metastases observed on DW-MRI according to the histopathological subtypes determined after surgical resection for lesions >1 cm in diameter

	Histopathological subtypes			
DW-MRI appearance at b=500 s mm^{-2}	Cellular	Necrotic	Fibrotic	Mixed
Rim	1	11	2	1
Uniform	1	0	2	1
Variegate	0	1	0	2

DW-MRI, diffusion-weighted MRI.

In our study, we found that colorectal liver metastases showed *rim* high signal intensity, *uniform* high signal intensity or *variegate* high signal intensity at a *b* value of 500 s mm^{-2} on DW-MRI. For metastases ≤1 cm in diameter, we found that the *uniform* pattern was most common, which may be difficult to distinguish from other solid liver lesions. However, for lesions >1 cm in diameter, the *rim* pattern was the most common, a feature which may aid the diagnosis of colorectal liver metastases in the appropriate clinical setting.

We found that the DW-MRI appearances of colorectal liver metastases could also reflect the underlying histopathology. In patients who underwent liver resection surgery for metastatic disease, the majority (11/15) of metastases >1 cm in diameter which exhibited the *rim* high signal intensity pattern on DW-MRI were found to contain significant central necrosis. As necrotic tissues showed less impeded water diffusion than cellular tumour tissues, the central necrotic area of a metastasis would therefore show greater MR signal attenuation than the more cellular tumour periphery, giving rise to the *rim* appearance on DW-MRI. The presence of necrosis in colorectal liver metastases is well described in the published literature. In one study, central coagulative necrosis was observed in 49% of liver metastases detected on T_2 weighted imaging [15]. In addition, pathologically proven necrotic tumour has also been shown to demonstrate lower signal intensity on high *b* value DW-MRI than viable tumour in an animal model [16].

In our study, the *uniform* and *variegate* high signal intensity patterns were associated with a variety of histological subtypes, making it difficult to draw conclusions about the pathological basis for these observations. However, we observed that, in metastases >1 cm in diameter, fibrotic or desmoplastic changes within the metastases may result in the *uniform* high signal intensity pattern or the *rim* high signal intensity, suggesting fibrosis

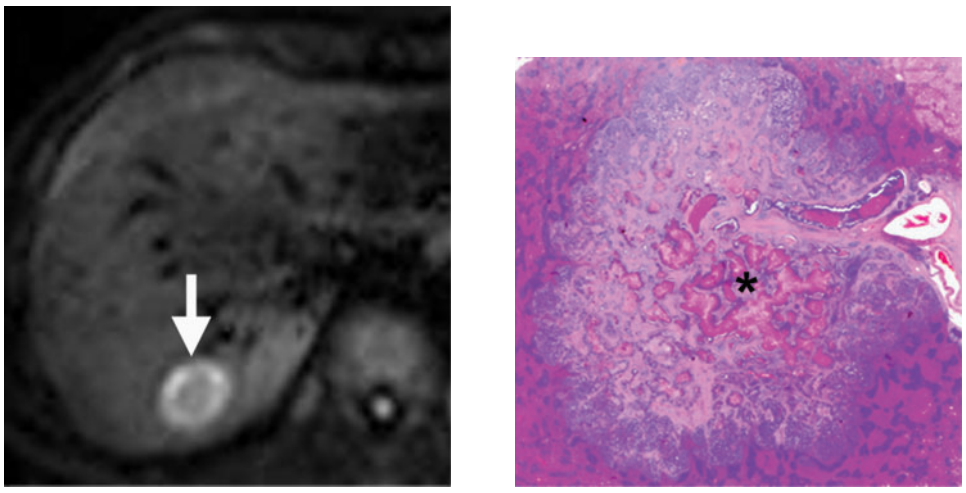

(a) (b)

Figure 3. A 57-year-old male with a solitary metastasis in the right lobe of the liver who underwent right segmentectomy surgery. (a) Diffusion-weighted MRI (echo time/repetition time=1850/60) acquired at a *b* value of 500 s mm^{-2} revealed a 3 cm metastasis in segment VII of the right lobe of the liver (arrow), which showed a rim high signal intensity pattern. (b) Haematoxylin and eosin-stained whole-mount histology section (2×) showed central necrosis (*) occupying more than 30% of the tumour area. The necrotic tissue was stained pinker than the cellular rim, which contained viable tumour cells and had a more purplish coloration. Note also a blood vessel supplying the metastasis.

may result in a varying extent of hindrance to water diffusion. This appears to be consistent with DW-MRI observations made of pathologically proven fibrosis in the body. For example, in patients with liver cirrhosis, hepatocellular swelling together with deposition of collagenous fibres is thought to hinder water diffusion, leading to less signal attenuation at DW-MRI and lower apparent diffusion coefficient (ADC) values [17, 18]. However, fibrotic stroma within an intrahepatic cholangiocarcinoma has also been shown to demonstrate a contrary appearance with greater signal attenuation at high *b* value DW-MRI and relatively high ADC value, mimicking an inflammatory pseudotumour [19]. Clearly, more research is needed to better understand DW-MRI signal alterations in fibrotic processes in the body.

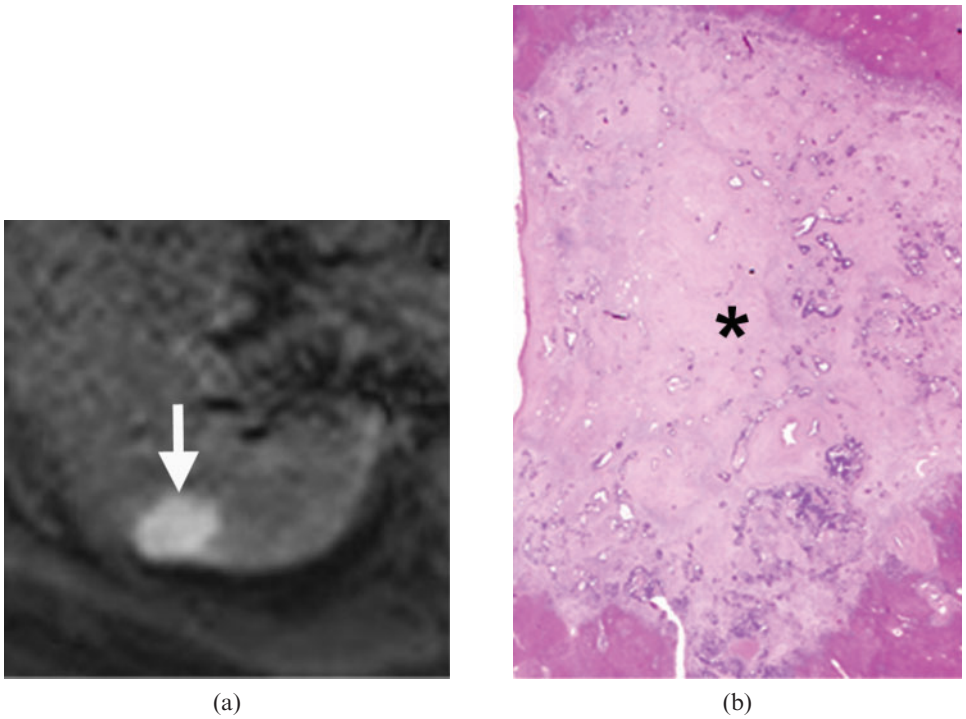

(a) (b)

Figure 4. A 64-year-old male with a metastasis in the right lobe of the liver treated with right hepatectomy. (a) Diffusion-weighted MRI (echo time/repetition time=1850/60) acquired at a *b* value of 500 s mm^{-2} demonstrated a 2.5 cm metastasis in segment VII of the right lobe of the liver (arrow), which showed uniform high signal intensity pattern. (b) Haematoxylin and eosin-stained histology section (2×) shows the tumour to be relatively acellular. The centre of the tumour showed an amorphous appearance (*) owing to collagen deposition. The tumour was classified as showing significant fibrotic change.

Interestingly, lesions ≤1 cm in diameter in our study frequently showed the *uniform* high signal intensity pattern. Possible hypotheses for this include: small metastases may be less susceptible to undergoing central necrosis and foci of necrosis within the small metastases may be beyond the spatial resolution of our current imaging to confidently detect.

There are limitations to our current study. First, the study was performed in a relatively small study population and only a proportion of patients underwent surgery to provide direct radiological–pathological comparison. Although we observed that the rim high signal intensity pattern was the most common appearance of colorectal liver metastases measuring >1 cm in diameter, and could relate this to underlying pathological changes, we were less successful in understanding the pathological basis for the *uniform* and *variegate* appearances on DW-MRI and further studies are warranted. Second, only qualitative evaluation of the DW-MRIs was performed in this study. We did not quantify the ADC value of the liver metastases. However, the ADC values of colorectal liver metastases have been published in the literature [20]. The mean ADC value of colorectal liver metastases was reportedly higher than that of normal liver [20], probably reflecting the high incidence of necrosis within the metastases. Third, there were no mucinous metastases found among our study population. Mucinous metastases may resemble cysts or haemangiomas on T_2 weighted imaging [21], and can in theory show signal suppression at b values of 500 s mm^{-2}, thus mimicking benign lesions. Future studies would help to establish the range of imaging appearances of mucinous metastases on DW-MRI.

Conclusion

Colorectal liver metastases exhibit three different morphological appearances on DW-MRI acquired at a b value of 500 s mm^{-2}. Metastases measuring >1 cm in diameter frequently exhibited a *rim* high signal intensity pattern, which could be explained by necrotic changes at histopathology.

References

1. Quillin SP, Atilla S, Brown JJ, Borrello JA, Yu CY, Pilgram TK. Characterization of focal hepatic masses by dynamic contrast-enhanced MR imaging: findings in 311 lesions. Magn Reson Imaging 1997;15:275–85.
2. Hamm B, Thoeni RF, Gould RG, Bernardino ME, Luning M, Saini S, et al. Focal liver lesions: characterization with nonenhanced and dynamic contrast material-enhanced MR imaging. Radiology 1994;190:417–23.
3. Furuhata T, Okita K, Tsuruma T, Hata F, Kimura Y, Katsuramaki T, et al. Efficacy of SPIO-MR imaging in the diagnosis of liver metastases from colorectal carcinomas. Dig Surg 2003;20:321–5.
4. Ward J, Guthrie JA, Wilson D, Arnold P, Lodge JP, Toogood GJ, et al. Colorectal hepatic metastases: detection with SPIO-enhanced breath-hold MR imaging—comparison of optimized sequences. Radiology 2003;228:709–18.
5. Kim KW, Kim AY, Kim TK, Park SH, Kim HJ, Lee YK, et al. Small (< or = 2 cm) hepatic lesions in colorectal cancer patients: detection and characterization on mangafodipir trisodium-enhanced MRI. AJR Am J Roentgenol 2004;182: 1233–40.
6. Koh DM, Brown G, Meer Z, Norman AR, Husband JE. Diagnostic accuracy of rim and segmental MRI enhancement of colorectal hepatic metastasis after administration of mangafodipir trisodium. AJR Am J Roentgenol 2007;188: W154–61.
7. Zech CJ, Herrmann KA, Reiser MF, Schoenberg SO. MR imaging in patients with suspected liver metastases: value of liver-specific contrast agent Gd-EOB-DTPA. Magn Reson Med Sci 2007;6:43–52.
8. Stern W, Schick F, Kopp AF, Reimer P, Shamsi K, Claussen CD, et al. Dynamic MR imaging of liver metastases with Gd-EOB-DTPA. Acta Radiol 2000;41:255–62.
9. Kim YK, Lee JM, Kim CS, Chung GH, Kim CY, Kim IH. Detection of liver metastases: gadobenate dimeglumine-enhanced three-dimensional dynamic phases and one-hour delayed phase MR imaging versus superparamagnetic iron oxide-enhanced MR imaging. Eur Radiol 2005;15: 220–8.
10. Le Bihan D, Turner R, Douek P, Patronas N. Diffusion MR imaging: clinical applications. AJR Am J Roentgenol 1992; 159:591–9.
11. Coenegrachts K, Delanote J, Ter Beek L, Haspeslagh M, Bipat S, Stoker J, et al. Improved focal liver lesion detection: comparison of single shot diffusion-weighted echo planar and single shot T_2 weighted turbo spin echo techniques. Br J Radiol 2007;80:524–31.
12. Parikh T, Drew SJ, Lee VS, Wong S, Hecht EM, Babb JS, et al. Focal liver lesion detection and characterization with diffusion-weighted MR imaging: comparison with standard breath-hold T_2-weighted imaging. Radiology 2008;246:812–22.
13. Nasu K, Kuroki Y, Nawano S, Kuroki S, Tsukamoto T, Yamamoto S, et al. Hepatic metastases: diffusion-weighted sensitivity-encoding versus SPIO-enhanced MR imaging. Radiology 2006;239:122–30.
14. Koh DM, Brown G, Riddell AM, Scurr E, Collins DJ, Allen SD, et al. Detection of colorectal hepatic metastases using MnDPDP MR imaging and diffusion-weighted imaging (DWI) alone and in combination. Eur Radiol 2008;18:903–10.
15. Outwater E, Tomaszewski JE, Daly JM, Kressel HY. Hepatic colorectal metastases: correlation of MR imaging and pathologic appearance. Radiology 1991;180:327–32.
16. Geschwind JF, Artemov D, Abraham S, Omdal D, Huncharek MS, McGee C, et al. Chemoembolization of liver tumor in a rabbit model: assessment of tumor cell death with diffusion-weighted MR imaging and histologic analysis. J Vasc Interv Radiol 2000;11:1245–55.
17. Taouli B, Tolia AJ, Losada M, Babb JS, Chan ES, Bannan MA, et al. Diffusion-weighted MRI for quantification of liver fibrosis: preliminary experience. AJR Am J Roentgenol 2007;189:799–806.
18. Girometti R, Furlan A, Bazzocchi M, Soldano F, Isola M, Toniutto P, et al. Diffusion-weighted MRI in evaluating liver fibrosis: a feasibility study in cirrhotic patients. Radiol Med (Torino) 2007;112:394–408.
19. Kitajima K, Shiba H, Nojiri T, Uwagawa T, Ishida Y, Ichiba N, et al. Intrahepatic cholangiocarcinoma mimicking hepatic inflammatory pseudotumor. J Gastrointest Surg 2007;11: 398–402.
20. Koh DM, Scurr E, Collins DJ, Pirgon A, Kanber B, Karanjia N, et al. Colorectal hepatic metastases: quantitative measurements using single-shot echo-planar diffusion-weighted MR imaging. Eur Radiol 2006;16:1898–905.
21. Lacout A, El Hajjam M, Julie C, Lacombe P, Pelage JP. Liver metastasis of a mucinous colonic carcinoma mimicking a haemangioma in T_2-weighted sequences. J Med Imag Radiat Oncol 2008;52:580–2.